Proceeding Paper

Nafion-Based Layer-by-Layer Coatings with Antimicrobial Activity [†]

Ella Gibbons [1],[*] , **Marta Krysmann** [2], **Spyridon Gavalas** [1] , **Kira Heslop** [1] **and Antonios Kelarakis** [1],[*]

1   School of Natural Sciences, University of Central Lancashire, Preston PR1 2HE, UK;
     sgavalas@uclan.ac.uk (S.G.); kheslop@uclan.ac.uk (K.H.)
2   School of Dentistry, University of Central Lancashire, Preston PR1 2HE, UK; mkrysmann@uclan.ac.uk
*   Correspondence: egibbons2@uclan.ac.uk (E.G.); akelarakis@uclan.ac.uk (A.K.)
†   Presented at the 4th International Online Conference on Nanomaterials, 5–19 May 2023;
     Available online: https://iocn2023.sciforum.net/.

Abstract: With the need for non-antibiotic approaches to microbial pathogenesis being ever present, the development of alternatives centred around infection prevention is of deep importance. Antimicrobial surface coatings offer a promising approach, as they can possess multiple favourable qualities such as low toxicity, longevity, and the capacity for re-coating. Of the possible coating methods, layer-by-layer (LbL) deposition provides a particularly useful approach, allowing for the facile creation of multilayered coatings on pre-existing surfaces. For these LbL coatings, Nafion, a synthetic polymer with excellent mechanical properties, was used as a stable foundation for two model trilayer systems. Both sets of systems comprised Nafion layered alongside compounds with well-established antimicrobial activity: lysozyme, chitosan, and carbon dots (CDots). In addition to their antimicrobial properties, lysozyme and chitosan are both nontoxic and biocompatible, making them ideal for biomedical applications. Similarly, CDots have low toxicity but also possess fluorescent properties, opening up the potential for the assessment of coating integrity, making these coatings suitable for high-wear surfaces. As such, the two trilayer systems were made of, respectively, Nafion, lysozyme, and chitosan; and Nafion, lysozyme, and CDots. When assessed against the representative Gram-negative and Gram-positive species *Escherichia coli* (*E. coli*) and *Staphylococcus aureus* (*S. aureus*), respectively, both trilayer systems showed excellent antimicrobial activity, producing up to 3 log reductions in colony-forming units compared with a control. The activity of both sets of systems, alongside the similar activity between systems, showed both good synergy between and interchangeability of layer components, opening up the possibility for further tailoring in future.

Keywords: antimicrobial; bilayer; carbon dots; chitosan; layer-by-layer; lysozyme; multilayer; Nafion; trilayer

1. Introduction

Antibiotic resistance constitutes an ever-present threat to global health, and in the face of a steadily ageing population and overburdened healthcare system, low-cost and effective approaches to infection prevention have never been more relevant.

Fomites constitute a major route for infection, with bacteria being capable of colonising most solid surfaces from door handles and public railings to air conditioning units and water lines [1]. Indwelling medical devices in particular, such as dental implants, prosthetic joints, and catheters, represent a particularly significant route for bacterial infection to take hold [2]. To combat this risk, surfaces may be imbued with antimicrobial properties such as adhesion prevention, "contact killing", and the release of bacteriostatic and/or bactericidal molecules [3]. Rather than creating an entirely new solid surface with antimicrobial properties, which may be cost prohibitive, an attractive approach is the coating of pre-existing surfaces. To this end, layer-by-layer (LbL) deposition is an appealing coating method due

to its facile and versatile nature [4]. LbL deposition is based primarily, but not exclusively, upon the adsorption of oppositely charged materials in an alternating fashion in order to create highly tuneable coatings, with both structure and composition controllable at a nanoscale level [5]. LbL systems may feature any number of materials, including enzymes, peptides, polymers, both metal- and carbon-based nanoparticles, and even antibiotics [6,7].

In this work, we are focusing on the use of four compounds to create LbL assemblies: Nafion, lysozyme, chitosan, and carbon dots (CDots). Nafion is an amphiphilic, negatively charged synthetic polymer comprising a polytetrafluoroethylene backbone with side chains of perfluorinated-vinyl-polyether and sulphonic acid end groups, most often used as part of proton exchange membranes. The polymer, however, also has documented biocompatibility and anti-biofilm activity [8,9]. Chitosan is a positively charged biopolymer comprising alternating units of N-acetylglucosamine and N-acetylmuramic acid, and has well-documented nontoxicity, biocompatibility, and antimicrobial activity. Chitosan has been used effectively for a range of purposes, including scaffolding for tissue regrowth, wound healing, and in antimicrobial films and coatings [10]. Lysozyme is a positively charged enzyme which, similarly to chitosan, has well-documented nontoxicity, biocompatibility, and antimicrobial activity. As such, lysozyme has been used for many of the same applications as chitosan such as wound healing and as part of various antimicrobial systems [11]. Lastly, CDots represent a large group of carbonaceous nanoparticles with a wide variety of applications, many based upon their excellent photoluminescent (PL) properties [12,13]. CDots can be derived in a cost-effective manner by means of thermal treatment of molecular precursors or crude biomass [14–16]. Due to a combination of PL and low toxicity, CDots show promise in the field of bioimaging, but also have applications in drug delivery, biosensing, as phototherapeutic agents, and in nano-forensics [17,18]. Similarly, the photosensitiser status of CDots, in addition to their small size, make them well suited for use as antimicrobials [19].

2. Materials and Methods

2.1. Materials

Nafion (DE 1021) with a total H+ exchange capacity of 1.1 mequiv/g was obtained from Chemous Company (Wilmington, DE, USA) as 10 wt% and 15 wt% dispersions in water (Ion-Power) and as a 15 wt% dispersion in a mixture of low-aliphatic alcohols (3-propanol, ethanol, etc.) (Ion-Power). Chicken egg white lysozyme (106 U/mg) (Buchs, St. Gallen, Switzerland) and medium-molecular-weight (MMW) chitosan (Milwaukee, WI, USA) were obtained from Sigma Aldrich (Dorset, UK). Chitosan was dispersed in distilled water containing 0.1 wt% acetic acid.

2.2. Contact Angle Measurements

Contact angle measurements were taken using an OptoSigma optical tensiometer (OptoSigma Corp. Santa Ana, CA, USA) using the standard sessile drop technique (Digidropmeter, GBX Scientific Ltd., Tallaght, Dublin, Republic of Ireland)Droplets (5 μL) of distilled water were deposited onto the coated quartz crystal and photos were captured 20 s after droplet deposition. A minimum of 5 droplets were measured for each specimen.

2.3. Circular Dichroism Spectrometry (CD)

The circular dichroism (CD) spectra of lysozyme solutions (0.01 mg) both with and without the presence of Nafion (0.01%) were measured using a J815 CD spectrapolarimeter (Jasco, Tokyo, Japan). Samples were placed into a quartz cuvette with a light path length of 0.1 cm and measured at 20 °C, 50 °C, and 80 °C. Each sample was run for 5 accumulations with a scanning range of 260–180 nm, a band width of 2 nm, data pitch 0.5 nm, digital integration time of 1 s, and a scanning speed of 100 nm/min. Values for the baseline (no cuvette) were subtracted automatically by the equipment. Values of the blank solution (ultrapure water) were subtracted manually using the software. Analysis of estimated secondary structure was carried out using DichroWeb [20,21].

2.4. Atomic Force Microscopy (AFM)

Measurements of the (quartz crystals) coated with desired layers were carried out using a Park XE-100 (Parksystems, Suwon, Republic of Korea) in non-contact mode using a cantilever with a spring constant close to 40 N/m. Images were taken at a scan rate between 0.2 and 0.5 Hz and at a 512-by-512-pixel resolution.

2.5. Antimicrobial Testing

A. A 25 mL broth was inoculated with a single loop of bacteria and incubated in a SciQuip Incu-Shake MIDI orbital shaker (SciQuip Ltd., Newtown, Shropshire, UK) set to 200 rpm and 37 °C for 24 h. Overnight cultures were washed and resuspended by the following means: cultures were centrifuged in an ALC PK 121R (ALC, Winchester, Virginia, USA) refrigerated centrifuge for 10 min at 4000 rpm. The supernatant was discarded, 20 mL 1/4 Strength Ringers solution was added, and the tube vortexed and then centrifuged again. After discarding the supernatant, cultures were resuspended in 2 mL 1/4 strength Ringers solution. Resuspended cultures were diluted to the equivalent of a 0.5 MacFarlane standard, measured using a Biochrom WPA 2800 visible spectrophotometer (BiocChrom Ltd., Cambridge, UK) set to 600 nm.

B. Quartz crystal microbalance with dissipation monitoring (QCM-D) was used to coat QCM-D crystals, also referred to here as discs. Disc testing was modified from a method in the pre-existing literature [8]. Discs used for antimicrobial testing were quartz crystals of diameter 150 nm (Control) and test discs were each assigned wells in a 12-well plate using a random number generator. Each well was lined with sterile aluminium foil for ease of removal and to prevent runoff. An additional well was filled with 1 mL sterile distilled water to prevent sample dehydration. Then, 200 µL of diluted, resuspended culture was added to each disc, before incubating at 37 °C for 20 h. Following incubation, discs and foil were transferred into 9.8 mL 1/4 strength Ringers solution and sonicated for 10 min. Sonicated solutions were serially diluted to 100 µL into 900 µL 1/4 strength Ringers solution several times. A total of 100 µL of each dilution was spread onto nutrient agar, with each dilution being plated in triplicate. Plates were incubated for 20 h at 37 °C in a static incubator then counted for colonies. Plates with 30–300 colonies were recorded alongside their respective dilution, and % decrease in test sample vs. control sample was calculated by: (Control-Test)/Control × 100.

3. Results and Discussion

As shown in Figure 1, water contact angles were found to be: Nafion 72.94°; $(Naf/Lys/CDot/Lys)_3$ 70.6°; $(Naf/CDot)_6$ 59.3°; and $(Naf/Lys)_6$ 45.29°. Discs coated with $(Naf/Lys/Naf/Chi)_2$ and $(Naf/Chi)_6$ were also evaluated, with contact angles of 58.92° and 64.08°, respectively. Although hydrophobic surfaces are generally seen as preferable, antimicrobial hydrophilic surfaces offer lower toxicity and thus greater application in biomedicine [22].

Figure 2 shows the roughness of the QCM-D discs coated with Nafion, $(Naf/Lys)_6$, $(Naf/CDot)_6$, and $(Naf/Lys/CDot/Lys)_3$. When coated onto a solid surface, lysozyme undergoes protein–surface interactions which render previously buried hydrophobic residues exposed, allowing for further interaction with other exposed hydrophobic residues, ultimately resulting in aggregation and cluster formation [24]. Nafion surface topography is largely due to the relative humidity and hydration level of the coating, with higher humidity decreasing the number but increasing the size of surface clusters [25]. The surface roughness of CDot layers can be affected by the number of hydrophilic groups of the particles, as well as the pH and ionic strength of the buffer used during deposition [26].
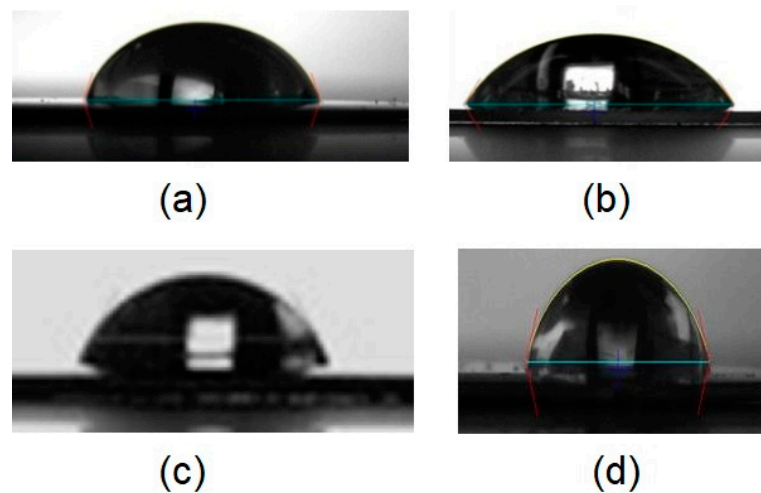
Figure 1. Contact angles of water on QCM-D discs coated with: (**a**) Nafion, (**b**) (Naf/Lys)$_6$, (**c**) (Naf/CDot)$_6$, and (**d**) (Naf/Lys/CDot/Lys)$_3$. Subscript number refers to the number of bi- or trilayers. (**a**,**b**) adapted from [23].
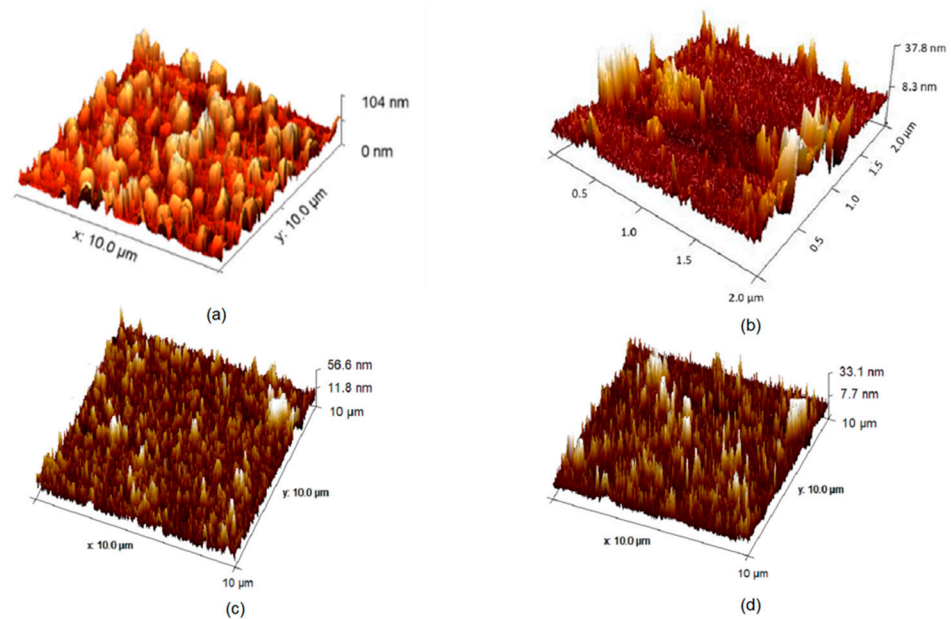
Figure 2. AFM of QCM-D crystals coated with: (**a**) Nafion, (**b**) (Naf/Lys)$_6$, (**c**) (Naf/CDot)$_6$, and (**d**) (Naf/Lys/CDot/Lys)$_3$. Subscript number refers to the number of bi- or trilayers. (**a**,**b**) adapted from [23].

Figure 3 shows a lawn of confluent bacteria for the control (uncoated QCM-D disc), compared with very few colonies of the coated test discs. Similar visuals are observed for the systems employing lysozyme and chitosan, with four systems achieving 4 log reductions in bacteria, suggesting strong synergy between components.

Figure 4 demonstrates the minimal disruption that Nafion complexation has on lysozyme secondary structures. As an intact binding site is necessary for cleavage of the 1,4 beta linkage between N-acetylmuramic acid (NAM) and N-acetyl-D-glucosamine (NAG) within the bacterial outer membrane, changes in secondary structure may negatively affect enzyme activity [27]. In addition to this, Nafion complexation produces a heat-protective effect, even beyond the denaturing temperature of 60 °C.

Figure 3. Agar spread plates of E. coli (**top**) and S. aureus (**bottom**). The leftmost photos were cultured on uncoated QCM-D crystals, while the rightmost photos were cultured on (Naf/CDot)$_6$-coated discs. Each control–test pair was taken at the same dilution.
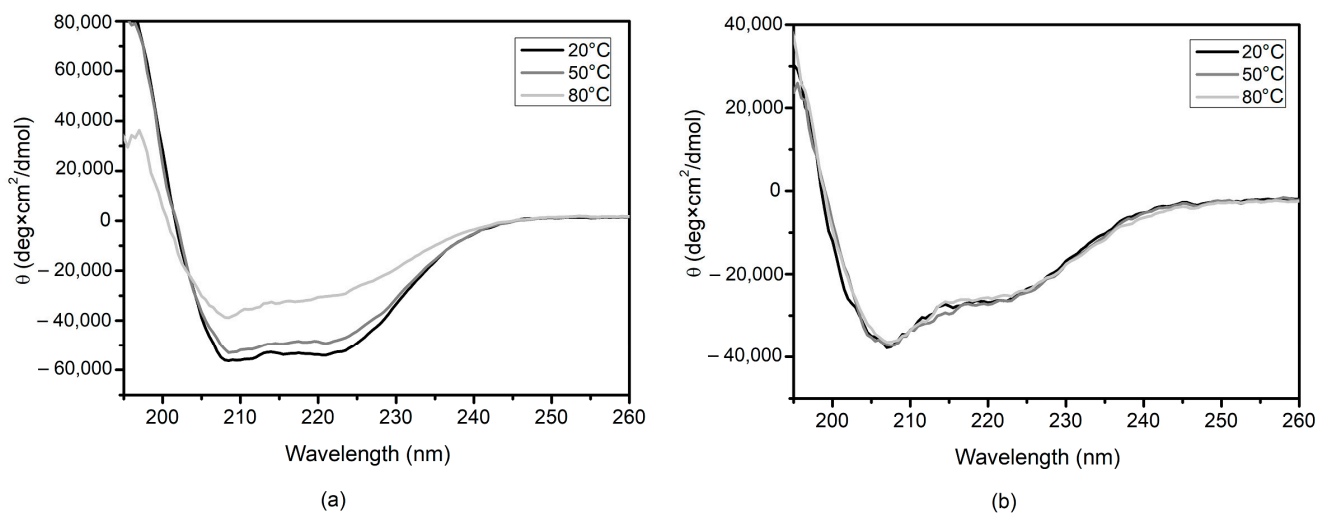

Figure 4. CD spectra for (**a**) lysozyme 0.01 mg and (**b**) lysozyme 0.01mg—Nafion 0.01%, heated from 20 °C to 80 °C in increments of 30 °C.

A primary approach to overcoming antimicrobial resistance is to employ systems with multiple mechanisms of action. Lysozyme, as mentioned previously, hydrolyses the β-1,4 bond between the NAG and NAM subunits of peptidoglycan. This activity is generally limited by the peptidoglycan being exposed in Gram-positive species, but not in Gram-negative species. However, it has been shown that when paired in systems alongside other compounds such as chitosan, the activity of lysozyme can be extended to Gram-negative species, particularly, *E. coli* [28]. The antimicrobial activity of chitosan is strongly

affected by level of deacetylation and molecular weight, with high deacetylation and low molecular weight being attributed to higher levels of activity [29]. Low-molecular-weight chitosan may enter the cell and disrupt metabolism by interacting with the negatively charged DNA to prevent the synthesis of mRNA and proteins [30]. Additionally, interaction between the positively charged polymer and negatively charged phospholipid bilayer may result in increased membrane permeability, leading to the leakage of critical cell components [31]. Chitosan has been shown to be effective against both Gram-negative and Gram-positive species, providing some explanation for its ability to broaden the spectrum of lysozyme's activity [32,33]. The activity of CDots is dependent upon a number of factors, including size, charge, and any surface functionalisation. The primary mechanism of antimicrobial activity is thought to be ROS generation, causing oxidative damage both to external cell walls and membranes, and to internal proteins and biomolecules, as well as DNA damage [34]. Both positively and negatively charged CDots are shown capable of eliciting antimicrobial activity, with negatively charged dots reported as being bacteriostatic and positively charged dots being bactericidal [35]. Nafion is documented as producing an exclusion zone, likely owing to its negative charge repelling the net negatively charged bacterial cell surface [35]. The exclusion zone is shown to be particularly effective against Gram-negative species, which generally possess a denser negative charge on the cell surface [36]. Negative charges are associated with repelling the net negatively charged bacteria, and are thus useful for anti-adhesive coatings [37,38]. Immobilised lysozyme has been associated with higher activity against Gram-negative bacteria owing to its more positive surface charge, which is in line with the results here [28].

4. Conclusions

In conclusion, we report on several model multilayer systems based the synergistic antimicrobials chitosan, lysozyme, CDots, and Nafion. It was shown that the chemical composition, wetting characteristics, and topological features were important parameters for producing strong antimicrobial activity. Our study demonstrates the potential of combining Nafion with more established antimicrobials for the creation of effective coatings against the ever-pressing threat of pathogenic bacterial colonisation.

Author Contributions: Conceptualisation, A.K.; methodology, E.G., M.K. and A.K.; validation, M.K. and A.K.; formal analysis, E.G. and S.G.; investigation, S.G., K.H. and E.G.; resources, M.K. and A.K.; data curation, S.G., K.H. and E.G.; writing—original draft preparation, E.G.; writing—review and editing, E.G. and A.K.; visualisation, E.G.; supervision, A.K. and M.K.; project administration, A.K.; funding acquisition, A.K. All authors have read and agreed to the published version of the manuscript.

Institutional Review Board Statement: Not applicable.

Informed Consent Statement: Not applicable.

Data Availability Statement: Data sharing not applicable.

Conflicts of Interest: The authors declare no conflict of interest.

References

1. Williams, J.F.; Johnston, A.M.; Johnson, B.; Huntington, M.K.; Mackenzie, C.D. Microbial contamination of Dental Unit waterlines: Prevalence, intensity and microbiological characteristics. *JADA* **1993**, *124*, 59–65. [CrossRef]
2. Flores-Mireles, A.L.; Walker, J.N.; Caparon, M.; Hultgren, S.J. Urinary tract infections: Epidemiology, mechanisms of infection and treatment options. *Nat. Rev. Microbiol.* **2015**, *13*, 269–284. [CrossRef] [PubMed]
3. Adlhart, C.; Verran, J.; Azevedo, N.F.; Olmez, H.; Keinänen-Toivola, M.M.; Gouveia, I.; Melo, L.F.; Crijns, F. Surface modifications for antimicrobial effects in the healthcare setting: A critical overview. *JHI* **2018**, *99*, 239–249. [CrossRef]
4. Michel, M.; Toniazzo, V.; Ruch, D.; Ball, V. Deposition mechanisms in layer-by-layer or step-by-step deposition methods: From elastic and impermeable films to soft membranes with ion exchange properties. *ISRN Mat. Sci.* **2012**, *2012*, 701695. [CrossRef]
5. Hammond, P.T. Form and Function in Multilayer Assembly: New Applications at the Nanoscale. *Adv. Mater.* **2004**, *16*, 1271–1293. [CrossRef]

6. Zhang, H.; Lu, H.; Hu, N. Fabrication of Electroactive Layer-by-Layer Films of Myoglobin with Gold Nanoparticles of Different Sizes. *J. Phys. Chem. B* **2006**, *110*, 2171–2179. [CrossRef] [PubMed]

7. Albright, V.; Zhuk, I.; Wang, Y.; Selin, V.; van de Belt-Gritter, B.; Busscher, H.J.; van der Mei, H.C.; Sukhishvili, S.A. Self-defensive antibiotic-loaded layer-by-layer coatings: Imaging of localized bacterial acidification and ph-triggering of antibiotic release. *Acta Biomater.* **2017**, *61*, 66–74. [CrossRef]

8. Zhong, L.J.; Pang, L.Q.; Che, L.M.; Wu, X.E.; Chen, X.D. Nafion coated stainless steel for anti-biofilm application. *Colloids Surf. B* **2013**, *111*, 252–256. [CrossRef]

9. Cheng, Y.; Moraru, C.I. Long-range interactions keep bacterial cells from liquid-solid interfaces: Evidence of a bacteria exclusion zone near Nafion surfaces and possible implications for bacterial attachment. *Colloids Surf. B* **2018**, *162*, 16–24. [CrossRef]

10. Zheng, W.; Chen, C.; Zhang, X.; Wen, X.; Xiao, Y.; Li, L.; Xu, Q.; Fu, F.; Diao, H.; Liu, X. Layer-by-layer coating of carboxymethyl chitosan-gelatin-alginate on cotton gauze for hemostasis and wound healing. *Surf. Coat. Technol.* **2021**, *406*, 126644. [CrossRef]

11. Chen, L.; Shi, W.; Zhang, T.; Zhou, Y.; Zhao, F.; Ge, W.; Jin, X.; Lin, W.; Guo, W.; Yin, D. Antibacterial activity of lysozyme-loaded cream against MRSA and promotion of scalded wound healing. *Int. J. Pharm.* **2022**, *627*, 122200. [CrossRef]

12. Kelarakis, A. Graphene quantum dots: In the crossroad of graphene, quantum dots and carbogenic nanoparticles. *COCIS* **2015**, *20*, 354–361. [CrossRef]

13. Kelarakis, A. From highly graphitic to amorphous carbon dots: A critical review. *MRS Energy Sustain.* **2014**, *1*, E2. [CrossRef]

14. Krysmann, M.J.; Kelarakis, A.; Dallas, P.; Giannelis, E.P. Formation mechanism of carbogenic nanoparticles with dual photoluminescence emission. *J. Am. Chem. Soc.* **2012**, *134*, 747–750. [CrossRef] [PubMed]

15. Stachowska, J.D.; Murphy, A.; Mellor, C.; Fernandes, D.; Gibbons, E.; Krysmann, M.; Kelarakis, A.; Burgaz, E.; Moore, J.; Yeates, S.G. A rich gallery of carbon dots based photoluminescent suspensions and powders derived by citric acid/ urea. *Sci. Rep.* **2021**, *11*, 10554. [CrossRef]

16. Krysmann, M.J.; Kelarakis, A.; Giannelis, E.P. Photoluminescent carbogenic nanoparticles directly derived from crude biomass. *Green Chem.* **2012**, *14*, 3141–3145. [CrossRef]

17. Fernandes, D.; Krysmann, M.J.; Kelarakis, A. Carbon dot based nanopowders and their application for fingerprint recovery. *Chem. Commun.* **2015**, *51*, 4902–4905. [CrossRef]

18. Verhagen, A.; Kelarakis, A. Carbon dots for forensic applications: A critical review. *Nanomater.* **2020**, *10*, 1535. [CrossRef]

19. Abu Rabe, D.I.; Mohammed, O.O.; Dong, X.; Patel, A.K.; Overton, C.M.; Tang, Y.; Kathariou, S.; Sun, Y.; Yang, L. Carbon dots for highly effective photodynamic inactivation of multidrug-resistant bacteria. *Mater. Adv.* **2020**, *1*, 321–325. [CrossRef]

20. Sreerama, N.; Woody, R.W. Estimation of protein secondary structure from circular dichroism spectra: Comparison of CONTIN, SELCON, and CDSSTR methods with an expanded reference set. *Anal. Biochem.* **2000**, *287*, 252–260. [CrossRef]

21. Whitmore, L.; Wallace, B.A. Protein secondary structure analyses from circular dichroism spectroscopy: Methods and reference databases. *Biopolymers* **2008**, *89*, 392–400. [CrossRef] [PubMed]

22. Ilker, M.F.; Nüsslein, K.; Tew, G.N.; Coughlin, E.B. Tuning the hemolytic and antibacterial activities of amphiphilic polynorbornene derivatives. *J. Am. Chem. Soc.* **2004**, *126*, 15870–15875. [CrossRef] [PubMed]

23. Gibbons, E.N.; Winder, C.; Barron, E.; Fernandes, D.; Krysmann, M.J.; Kelarakis, A.; Parry, A.V.; Yeates, S.G. Layer by layer antimicrobial coatings based on Nafion, lysozyme, and Chitosan. *Nanomaterials* **2019**, *9*, 1563. [CrossRef] [PubMed]

24. Kim, D.T.; Blanch, H.W.; Radke, C.J. Direct imaging of lysozyme adsorption onto mica by atomic force microscopy. *Langmuir* **2002**, *18*, 5841–5850. [CrossRef]

25. James, P.J.; Elliott, J.A.; McMaster, T.J.; Newton, J.M.; Elliott, A.M.; Hanna, S.; Miles, M.J. Hydration of Nafion® studied by AFM and X-ray scattering. *J. Mater. Sci.* **2000**, *35*, 5111–5119. [CrossRef]

26. da S. Pinto, T.; Alves, L.A.; de Azevedo Cardozo, G.; Munhoz, V.H.O.; Verly, R.M.; Pereira, F.V.; de Mesquita, J.P. Layer-by-layer self-assembly for Carbon Dots/Chitosan-based multilayer: Morphology, thickness and molecular interactions. *Mater. Chem. Phys.* **2017**, *186*, 81–89.

27. Kirby, A. The lysozyme mechanism sorted—After 50 years. *Nat. Struct. Mol. Biol.* **2001**, *8*, 737–739. [CrossRef]

28. Jiang, S.; Qin, Y.; Yang, J.; Li, M.; Xiong, L.; Sun, Q. Enhanced antibacterial activity of lysozyme immobilized on chitin nanowhiskers. *Food Chem.* **2017**, *221*, 1507–1513. [CrossRef]

29. Omura, Y.; Shigemoto, M.; Akiyama, T.; Saimoto, H.; Shigemasa, Y.; Nakamura, I.; Tsuchido, T. Antimicrobial Activity of Chitosan with Different Degrees of Acetylation and Molecular Weights. *Biocontrol. Sci.* **2003**, *8*, 25–30. [CrossRef]

30. Zheng, L.; Zhu, J. Study on antimicrobial activity of chitosan with different molecular weights. *Carbohydr. Polym.* **2003**, *54*, 527–530. [CrossRef]

31. Li, X.; Feng, X.; Yang, S.; Fu, G.; Wang, T.; Su, Z. Chitosan kills Escherichia coli through damage to be of cell membrane mechanism. *Carbohydr. Polym.* **2010**, *79*, 493–499. [CrossRef]

32. Coma, V.; Deschamps, A.; Martial-Gros, A. Bioactive packaging materials from edible chitosan polymer—Antimicrobial activity assessment on dairy-related contaminants. *J. Food Sci.* **2003**, *68*, 2788–2792. [CrossRef]

33. Chung, Y.C.; Su, Y.P.; Chen, C.C.; Jia, G.; Wang, H.L.; Wu, J.C.; Lin, J.G. Relationship between antibacterial activity of chitosan and surface characteristics of cell wall. *Acta Pharm. Sin. B* **2004**, *25*, 932–936.

34. Li, H.; Huang, J.; Song, Y.; Zhang, M.; Wang, H.; Lu, F.; Huang, H.; Liu, Y.; Dai, X.; Gu, Z.; et al. Degradable carbon dots with broad-spectrum antibacterial activity. *ACS Appl. Mater. Interfaces.* **2018**, *10*, 26936–26946. [CrossRef]

35. Bing, W.; Sun, H.; Yan, Z.; Ren, J.; Qu, X. Programmed Bacteria Death Induced by Carbon Dots with Different Surface Charge. *Small* **2016**, *12*, 4713–4718. [CrossRef]
36. Klyuzhin, I.; Symonds, A.; Magula, J.; Pollack, G.H. New Method of Water Purification Based on the Particle-Exclusion Phenomenon. *Environ. Sci. Technol.* **2008**, *42*, 6160–6166. [CrossRef] [PubMed]
37. Wilhelm, M.J.; Sharifian, G.; Wu, T.; Li, Y.; Chang, C.; Ma, J.; Dai, H. Determination of bacterial surface charge density via saturation of adsorbed ions. *Biophys. J.* **2021**, *120*, 2461–2470. [CrossRef] [PubMed]
38. Terada, A.; Okuyama, K.; Nishikawa, M.; Tsuneda, S.; Hosomi, M. The effect of surface charge property on escherichia coli initial adhesion and subsequent biofilm formation. *Biotechnol. Bioeng.* **2012**, *109*, 1745–1754. [CrossRef]